Numerical Simulations of Xenon Diffusive Exchange in Human Lung Tissue and Capillaries using Geometrical Models Based on Histology Sections

Neil James Stewart[1], Juan Parra-Robles[1], and Jim Michael Wild[1]
[1]*Academic Unit of Radiology, University of Sheffield, Sheffield, South Yorkshire, United Kingdom*

Target Audience: Hyperpolarized gas and diffusion MRI communities; respiratory scientists and physiologists.

Introduction & Purpose: NMR spectroscopy and imaging of hyperpolarized (HP) ^{129}Xe in the lungs has been shown to be an effective non-invasive probe of pulmonary gas exchange, utilizing xenon's solubility in parenchyma and blood, and the wide chemical shift range of the ^{129}Xe resonance (~ 200 ppm in vivo). The chemical shift saturation recovery (CSSR) spectroscopy method was developed to study the temporal dynamics of xenon exchange from alveoli to pulmonary capillaries using HP ^{129}Xe [1, 2]. ^{129}Xe CSSR uptake data can be modelled with the diffusion equations to extract quantitative information about lung microstructure and gas exchange, which has enabled the measurement of alveolar septal thickening in pulmonary fibrosis (PF) with ^{129}Xe MR [1, 3]. Existing analytical models of diffusional gas transfer have been limited to simple one-dimensional geometries assuming uniform alveolar septal thickness (d) [1], tissue thickness [2, 4] and an identical diffusion coefficient of xenon in lung tissue and blood (~ $3.3\text{x}10^{-6}\text{cm}^2\text{s}^{-1}$) [5]. In addition, preliminary numerical simulations have been implemented for a single alveolus considering uniform tissue thickness [6]. In this work, 2D finite element (FEM) analysis of xenon diffusive exchange NMR in the alveoli, pulmonary tissues and capillaries was performed using 3D cylindrical models and realistic alveolar geometries derived from 2D human lung histology sections.

Methods: FEM simulations of xenon diffusion in the human lungs were implemented in COMSOL Multiphysics (Burlington, MA) considering two geometrical situations: i) single capillaries were represented by uniform thickness cylinders (diameter, d = 10 µm), with a tissue lumen layer of variable thickness (δ) sheathing part of the cylinder, as shown in Fig 1a. The equations of diffusion (tissue) and diffusion-convection (blood) were solved for different values of δ, blood flow velocity, v, and tissue diffusion coefficient, D_t for this geometry. ii) 2D histological sections of the lung alveoli [7] were segmented, converted to binary images and imported into COMSOL. In order to simulate the effect of interstitial lung fibrosis, alveolar septa were artificially-thickened. For all geometries, simulations were run from time t = 0 (with initial dissolved and gaseous xenon longitudinal magnetizations of zero and one, respectively), to t = 0.75 s, with a time-step of 0.001 s. Boundary conditions between media were defined based on conservation of flux and the xenon partition coefficient in each medium.

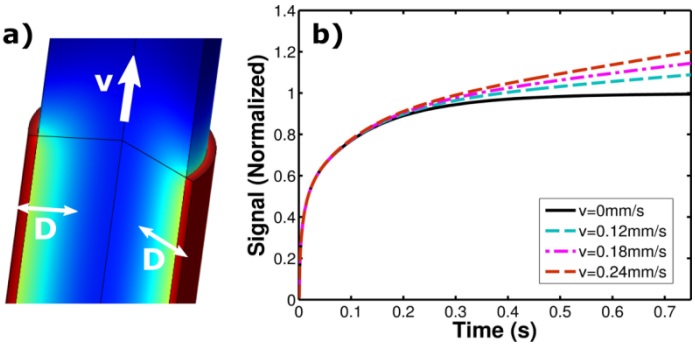

Figure 1: a) Snapshot of xenon diffusion in the uniform cylinder representation (time, t = 60 ms). b) Simulated dissolved ^{129}Xe signal using the cylinder representation with different blood flow velocities (v).

Results & Discussion: Fig 1a illustrates the simulated distribution of xenon magnetization in a pulmonary capillary (cylinder) after 60 ms, highlighting the rapid saturation of the tissue layer with polarized xenon from the gas reservoir (red). Fig 1b shows simulated xenon "uptake curves" of the predicted MR signal in a CSSR experiment. These were generated by integrating the total xenon magnetization from the cylinder geometry for different blood flow velocities, and clearly exhibit the "partial time effect" measured in vivo [1, 2]. In addition, simulations for different δ and D_t demonstrated subtle changes in the shape of the uptake curve, indicating that small changes in septal thickness, cardiac output, or lung tissue composition may be difficult to uniquely identify from ^{129}Xe CSSR data since different combinations of these effects can produce similar signal dynamics. Fig 2 illustrates the xenon diffusion dynamics in the 2D histology-derived geometry (a), and one with artificially-thickened septa (b). The lung tissue and capillaries in (a) were rapidly saturated with xenon from the alveoli in a similar manner to that observed for the cylinder geometry with uniform d = 10 µm.

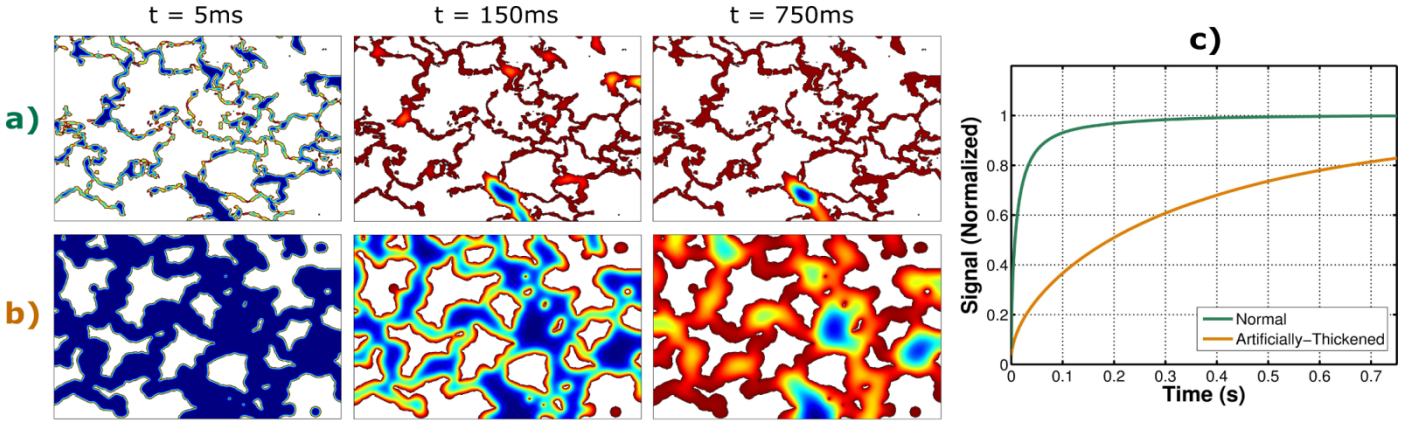

Figure 2: a) Distribution of xenon dissolved in parenchymal tissues and capillaries at three different time-points (5 ms, 150 ms and 750 ms) using a 2D geometry derived from normal lung histology. b) Distribution of dissolved xenon at the same three time-points for artificially-thickened alveolar septa. c) Simulated time-dependence of the total dissolved ^{129}Xe MR signal, integrated over the entire 2D domain, for both geometries.

However, the simulated uptake curve for the histology geometry (Fig 2c) exhibits a slightly different profile to the case of a uniform thickness model, due to the wide distribution of thicknesses present. As expected, the artificially-thickened septa (Fig 2b) required a considerably longer time to saturate than normal tissues, indicating a change from "perfusion-limited" to "diffusion-limited" gas exchange. Although the resulting signal dynamics (Fig 2c) do not exhibit the same shape as that measured in PF by ^{129}Xe CSSR [3], the inclusion of blood flow and the use of real histology sections from PF lung tissue will likely yield better agreement.

Conclusion: FEM simulations of xenon diffusion in the human alveolar spaces, lung parenchyma and blood have been performed using segmented 2D histology sections to provide realistic geometries. In addition, the effect of pulmonary perfusion has been simulated by considering the capillaries as uniform thickness cylinders. This work has implications for future MR imaging and spectroscopy studies with dissolved ^{129}Xe in the lungs, in terms of choice of acquisition timing parameters, and in particular, to improve the accuracy of modelling of lung microstructure and gas exchange with dissolved ^{129}Xe lung NMR techniques.

References: [1] S. Patz et al., New J Phys. 2011;13:015009. [2] Y. V. Chang et al., MRM. 2013;69:884-890. [3] N. J. Stewart et al., MRM. 2014; doi:10.1002/mrm.25400. [4] S. Månsson et al., MRM. 2003;50:1170-1179. [5] K. Ruppert et al., MRM. 2004;51:676-687. [6] O. Doganay et al., In: Proc ISMRM, 2014; Milan, Italy. [7] F. N. Miller and Uniformed Services University of the Health Sciences (http://histology-world.com).